

# Simulation of the annual and diurnal cycles of rainfall over South Africa by a regional climate model

Benjamin Pohl · Mathieu Rouault · Shouraseni Sen Roy

Received: 25 June 2013 / Accepted: 30 December 2013 / Published online: 10 January 2014  
© Springer-Verlag Berlin Heidelberg 2014

**Abstract** The capability of a current state-of-the-art regional climate model for simulating the diurnal and annual cycles of rainfall over a complex subtropical region is documented here. Hourly rainfall is simulated over Southern Africa for 1998–2006 by the non-hydrostatic model weather research and forecasting (WRF), and compared to a network of 103 stations covering South Africa. We used five simulations, four of which consist of different parameterizations for atmospheric convection at a  $0.5 \times 0.5^\circ$  resolution, performed to test the physic-dependency of the results. The fifth experiment uses explicit convection over tropical South Africa at a  $1/30^\circ$  resolution. WRF simulates realistic mean rainfall fields, albeit wet biases over tropical Africa. The model mean biases are strongly modulated by the convective scheme used for the simulations. The annual cycle of rainfall is well simulated over South Africa, mostly influenced by tropical summer rainfall except in the Western Cape region experiencing winter rainfall. The diurnal cycle shows a timing bias, with

atmospheric convection occurring too early in the afternoon, and causing too abundant rainfall. This result, particularly true in summer over the northeastern part of the country, is weakly physic-dependent. Cloud-resolving simulations do not clearly reduce the diurnal cycle biases. In the end, the rainfall overestimations appear to be mostly imputable to the afternoon hours of the austral summer rainy season, i.e., the periods during which convective activity is intense over the region.

**Keywords** Regional climate modeling · Rainfall · Diurnal cycle · Annual cycle · Atmospheric convection · South Africa

## 1 Introduction

Due to its subtropical location, its marked topography and the influence of two contrasted ocean currents, South Africa experiences a complex climate, under the influence of both tropical convection and mid-latitude dynamics. These particularities imply that spatial and temporal distribution of rainfall develops small-scale features that are generally not well represented by coarse-resolution general circulation models (GCM). Yet, predicting rainfall (in time and space) is of primary importance for the region, due to the predominance of rain-fed agriculture. The semi-arid conditions over most parts of the country make water resource a limiting factor for agronomic yields: large departures in the seasonal rainfall amounts (either drought or floods) can have particularly detrimental effects on the economies and societies of the region (Mason and Jury 1997; Reason and Jagadheesha 2005).

In recent years, many studies used this fine-resolution regional climate models (RCM) to investigate climate

---

B. Pohl (✉)  
Centre de Recherches de Climatologie,  
UMR6282 Biogéosciences, CNRS/University of Burgundy,  
6 Boulevard Gabriel, 21000 Dijon, France  
e-mail: benjamin.pohl@u-bourgogne.fr

M. Rouault  
Department of Oceanography, Mare Institute,  
University of Cape Town, Cape Town, South Africa

M. Rouault  
Nansen-Tutu Center for Marine Environmental Research,  
University of Cape Town, Cape Town, South Africa

S. S. Roy  
Department of Geography and Regional Studies,  
University of Miami, Coral Gables, FL 33124, USA

variability or predictability over Southern Africa, allowing for a more detailed regionalization (e.g., Joubert et al. 1999; Engelbrecht et al. 2002; Tadross et al. 2006; Kgatuke et al. 2008; Williams et al. 2010; Crétat et al. 2011; Ratnam et al. 2012; Vignaud et al. 2012). Even though all ranges of climate variability are not realistically reproduced (Boulard et al. 2013) and uncertainties due to the model physics and/or internal variability are strong (Crétat et al. 2012; Crétat and Pohl 2012; Ratna et al. 2013), these works contributed to show that RCM are indeed more efficient than GCM to take into account rainfall anisotropy and local to regional climate properties.

Both the diurnal and annual cycles, i.e., the two “natural” cycles forced by insolation, show some spatial complexity over the region. On the one hand, the climatology of South African rainfall is well documented. The southwestern tip of the country experiences dominant austral winter rainfall, mostly due to mid-latitude influence; further east along the South Coast wet conditions prevail throughout the year, in line with local effects of the warm Agulhas Current system (e.g., Rouault et al. 2002, 2003) and of the orography. The northwestern part of South Africa is more arid, at the periphery of the Kalahari/Namib Desert, forming a strong zonal gradient with the eastern and northeastern regions, where summer rainfall is prevalent due to an increasing influence of deep tropical convective processes. On the other hand, the diurnal cycle of rainfall was recently shown to be equally complex (Rouault et al. 2013), with distinct behaviors (timing and amplitude) between the hinterland and the coastal regions submitted to oceanic influence. Due to their spatial heterogeneity, and their strong association with surface conditions, such features of the South African climate require high-resolution climate simulations to be properly captured by climate models. Yet, to date, no study attempted to evaluate how they can be simulated at fine spatial and temporal scales, a gap that the present work aims to fill.

Previous work showed that numerical climate models (either global or regional) often produce satisfactory seasonal cycles of rainfall, but are less efficient to reproduce the intrinsic properties of the diurnal cycle, especially where convective rainfall predominate. Over the western Amazonia basin, Betts and Jakob (2002) found that precipitation start a few hours too early in the ECMWF model, because their model does not simulate well the morning growth of the non-precipitating convective boundary layer. Over the United States, Dai et al. (1999) obtained too weak diurnal cycles of rainfall using the RegCM regional model parameterized with three different convective schemes, partly due to too much cloudiness and too weak criteria used to initiate convection, hereby causing the convection to occur too early and explaining the overestimation (underestimation) of precipitation frequency (intensity). At

the global scale, Dai and Trenberth (2004) show that the CCSM2 GCM simulates a too large contribution of convective rainfall to total amounts. They stress that convective activity is also initiated too early in their model, preventing convective available potential energy from accumulating and resulting thus in too weak convection in the afternoon. More recently, over eastern Australia, Evans and Westra (2012) showed that the WRF model does a rather good job for simulating the diurnal cycle of rainfall. Its spatial variability was accurately simulated, but its amplitude was overestimated during the warm season. They obtained also rather realistic amounts and timing of rainfall peaks (in spite of too many simulated rainy days of too low intensity). This issue has also been addressed recently in the framework of the CORDEX-Africa regional modeling exercise. Although most models accurately succeed at simulating the annual cycle of rainfall at the continental scales (Hernandez-Diaz et al. 2013; Nikulin et al. 2012), current RCM were shown to have some difficulties at simulating the diurnal cycle, which are mostly attributable to convective parameterizations (Nikulin et al. 2012). However, the RCM using KF convection seems to simulate more realistic diurnal cycles (*ibid.*).

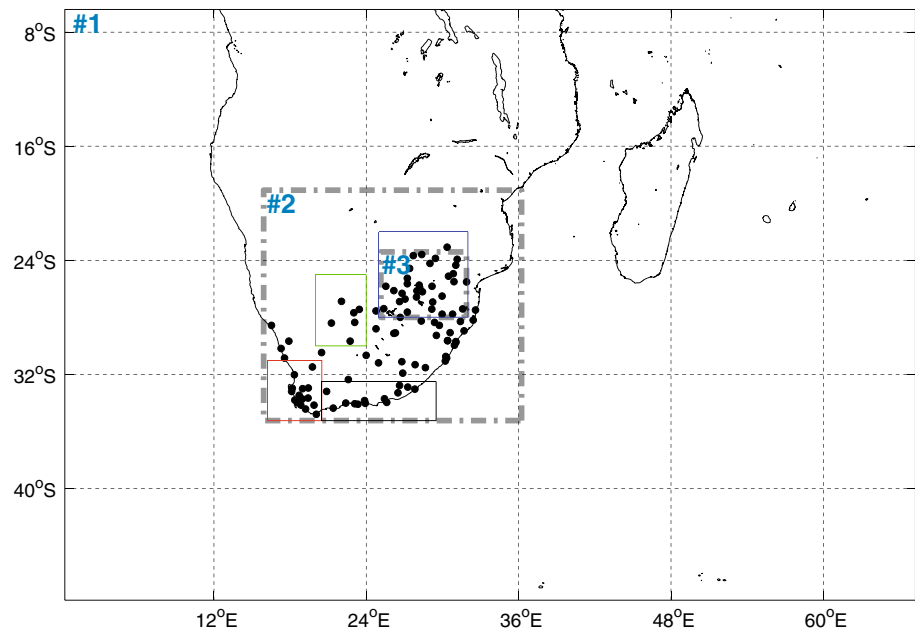
Motivated by these results, the aim of the present study is twofold:

- explore how the seasonal and diurnal cycles of rainfall are simulated by a current state-of-the-art non-hydrostatic RCM over South Africa;
- assess the sensitivity of the results to the horizontal resolution and to the representation of atmospheric convection, by considering successively three parameterizations and by resolving atmospheric processes explicitly over a targeted area.

This work is also a good opportunity to reinvestigate the model biases over the region in more detail than former modeling studies, that did not document how the model errors are distributed in time and space (i.e., in which months or hours of the day largest biases are concentrated: Crétat et al. 2012, Ratnam et al. 2012) and mostly considered the only austral summer rainy season (Vignaud et al. 2012; Boulard et al. 2013). Over South Africa, such evaluation is made possible by a relatively dense network of rain-gauge stations available at the hourly timescale over a 10-year period.

This paper is organized as follows. Section 2 presents the observational datasets used to evaluate model outputs, as well as the model used for this work and the associated experimental set-up. Section 3 presents the model mean biases and its skill for simulating the annual and diurnal cycles, as well as the physics-dependency and sensitivity to the spatial resolutions. Main results are then summarized and discussed in Sect. 4.

**Fig. 1** Simulation domain, map of the rain gauge records available over South Africa (black circles) and regional domains used to calculate the rainfall indices (Northeast: blue box; Northern Cape: green box; Western Cape: red box; South Coast: black box). The dashed grey rectangles show the nested domains used for the N3 experiment, with the domain names labeled in the upper left-hand corners



## 2 Data and experimental set-up

Observed rainfall is derived from hourly records available for 103 stations between 1998 and 2006, already used in Rouault et al. (2013). Following the World Meteorological Organization's standards, raw data were converted into UTC (coordinated universal time) series, the South African Standard Time (SAST) being 2 h ahead of UTC. Four regional indices (Fig. 1) are calculated and correspond to the northeastern part of South Africa, the Northern Cape, the Western Cape and the South Coast. For the large scale, Southern Africa and surrounding ocean, we are using the  $1^\circ \times 1^\circ$  resolution daily GPCP-1dd product (Huffman et al. 2001).

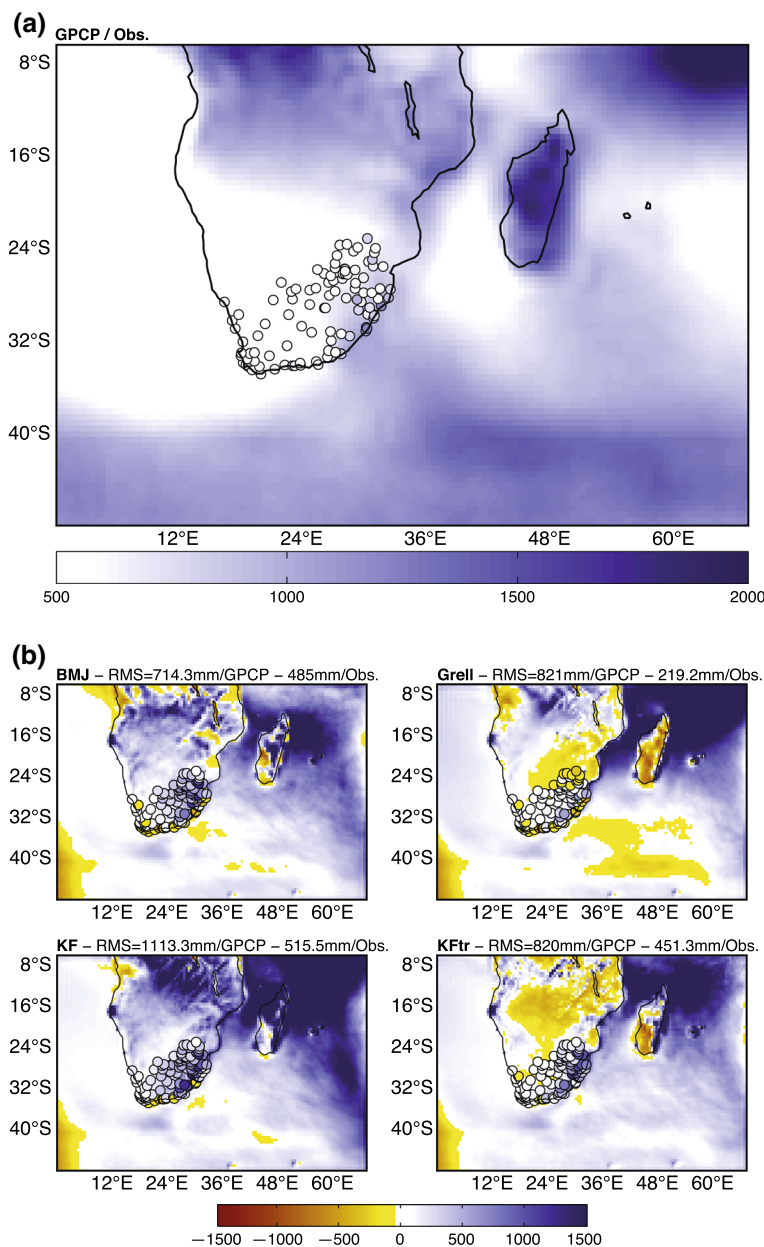
Five regional simulations are performed using the non-hydrostatic weather research and forecasting/advanced research WRF (ARW) model, version 3.3.1 (WRF hereafter, Skamarock et al. 2008). All simulations are carried out over the domain  $0^\circ$ – $68^\circ$ W,  $5^\circ$ S– $48^\circ$ S ( $146 \times 96$  grid-points, with a  $2.5^\circ$  buffer zone out of the domain to prescribe lateral boundary conditions), shown in Fig. 1 and referred to as domain #1. The spatial resolution is set at  $0.5^\circ$  (roughly 55 km), with 28 levels on the vertical. Simulations are initialized on January 1st 1997 with one-year long spin-up, with model outputs (rainfall) archived at the daily (hourly) timescale over 1998–2006.

The physical package includes the WSM 6-class graupel scheme for cloud microphysics (Hong and Lim 2006) and the Yonsei University parameterization of the Planetary Boundary Layer (PBL; Hong et al. 2006). Radiative transfer is parameterized with the Rapid Radiative Transfer Model scheme (Mlawer et al. 1997) for long waves and

Dudhia (1989) scheme for short waves. Over the continents WRF is coupled with the 4-layer NOAH land surface model (Chen and Dudhia 2001a, b). Surface data are taken from United States Geological Survey (USGS) database, which describes a 24 category land-use index based on climatological averages, and a 17 category United Nations Food and Agriculture Organization soil data, both available at 10 arc minutes. The four simulations only differ by their convective scheme [Betts–Miller–Janjic for exp. BMJ (Betts 1986; Betts and Miller 1986; Janjic 1994), Grell–Dévényi for exp. Grell (Grell 1993; Grell and Dévényi 2002), Kain–Fritsch for KF (Kain 2004), and Kain–Fritsch using the modified trigger function based on moisture advection and developed by Ma and Tan (2009) for exp. KFtr]. N3 experiments uses two additional one-way nested domains (referred to as domains #2 and #3), respectively centered over South Africa and the northeastern part of the country (Gauteng, Limpopo and Mpumalanga provinces), with horizontal resolutions fixed at  $1/6^\circ$  ( $\sim 18.3$  km,  $133 \times 112$  grid-points) and  $1/30^\circ$  ( $\sim 3.6$  km,  $206 \times 156$  grid-points). Atmospheric convection is parameterized using KFtr settings for the two largest domains (#1–2), and is explicitly resolved in domain #3. The use of one-way (consisting in a forcing of the nested domains by their parent domain) instead of two-way nesting (consisting in a feedback between the nested and the parent domains) allows comparison between the solutions of the respective domains over their common regions, and thus allows addressing the sensitivity of the results to the model resolution.

Forcing data is provided every 6 h by ERA-Interim reanalyses (Simmons et al. 2007; Dee et al. 2011) at a  $1.5^\circ$

**Fig. 2** **a** Annual mean rainfall amount (mm), 1998–2006, according to GPCP-1dd and rain gauge records. **b** WRF mean biases. RMS errors against GPCP-1dd and rain gauge records are labeled on the figure



horizontal resolution and 19 pressure levels. SST fields are prescribed every 24 h after a linear interpolation of monthly ERA-Interim SST.

### 3 Results

#### 3.1 Model mean climate and biases

Figure 2a shows the 1998–2006 annual mean rainfall amounts over the simulation domain, together with in situ measurements over South Africa. Largest rainfall amounts are clearly located at the very low latitudes in the northern part of the domain, which correspond to deep tropical

convection embedded in the Inter-Tropical Convergence Zone (ITCZ). Wet conditions also prevail over Madagascar, due to orographic lifting sustaining atmospheric instability, and to a lesser extent in the mid-latitudes, due to mid-latitude baroclinic transient perturbations. Southern Africa is much drier, especially its western parts close to the Southern Atlantic, where atmospheric stability is favored by the Saint-Helena high-pressure system that leads to both dry condition and strong upwelling favorable wind along the coast. The eastern part is wetter, especially along a NW–SE oriented band linking the continent and the SW Indian Ocean and referred to in the literature as the South Indian Convergence Zone (SICZ, Cook 2000), mostly active during the austral summer season.

Figure 2b shows the bias between GPCP-1dd, observation (circle) and WRF for the 4 convective schemes presented in Sect. 2. WRF over-estimates rainfall amounts over the tropical Indian Ocean and tropical Africa (except for KFtr experiment using the Ma and Tan (2009) moisture-advection based trigger function). In Southern Africa, the BMJ and KF convective schemes produce too wet conditions, while the situation is more contrasted with Grell and KFtr. RMS (root-mean-square) errors are smaller for South Africa against observation, than for the whole domain against GPCP-1dd. The smallest (largest) large-scale biases are obtained with BMJ (KF) convection at the domain scale; for South Africa Grell (KF) is the most (less) realistic. This confirms the results of Cr  tat et al. (2012), however obtained for a single austral summer rainy season representative of the climatology, and more recently Ratna et al. (2013). Biases in the simulated moisture fluxes and convergence over Southern Africa were previously found to be mainly responsible for WRF errors over the region (Cr  tat et al. 2012, Vigaud et al. 2012, Ratnam et al. 2012). Ratna et al. (2013) also discussed the too stable (unstable) atmospheric conditions associated with GD (KF) scheme over South Africa. In this study, we point out the predominant influence of the trigger function, KFtr scheme strongly reducing the rainfall overestimations produced by KF (Fig. 2b). Additional analyses (not shown) reveal that this improvement is mostly due to a decrease of the number of simulated rainy days ( $>1 \text{ mm day}^{-1}$ ), hereby favoring more realistic probability density functions of the simulated daily rainfall.

The model also allows separating convective and stratiform rainfall (respectively produced by convective and cloud microphysics schemes). At the domain and South African scales the contribution of convective rainfall to total amounts is shown in Table 1 for the austral summer (November through March) and winter (May through July) seasons. These seasons were also used in Rouault et al. (2013) and Philippon et al. (2012), respectively, and correspond to the core of the rainy seasons in summer for subtropical South Africa, and in winter for the Western Cape region. All schemes provide results that are consistent with ERA-Interim rainfall. From one scheme to another, sizeable differences can also be found. For instance, the Grell scheme tends to produce the largest fractions of convective rainfall in both seasons, especially over South Africa in summer, while KFtr simulates sensibly less convective rainfall than KF. This shows that the simulated rainfall amounts and the contribution of convective rainfall are not directly related: Grell (KFtr) produce rather dry (realistic) conditions over South Africa, with rainfall resulting mainly (weakly) from atmospheric convection. This illustrates that the model biases are not solely imputable to the rainfall amounts simulated by the

**Table 1** Relative contribution (%) of convective rainfall to seasonal rainfall amounts for the austral summer (November through March, first line of each cell) and austral winter season (May through July, second line) averaged spatially over the whole simulation domain and the South African domain

NDJFM MJJ	Simulation domain [0–67°W, 5–45°S]	South Africa [15–35°W, 21–36°S]
ERA-Interim	60.6	67.4
	45.1	71.0
BMJ	41.7	51.2
	53.3	50.5
Grell	59.1	73.8
	56.3	59.6
KF	47.4	63.3
	54.6	62.7
KFtr	44.6	50.7
	47.2	46.4

convective schemes, but also depend on interactions between these schemes and cloud microphysics. Although the results presented in this section mostly confirm previous studies, it may now be questioned how these biases vary over the seasonal and diurnal cycles.

### 3.2 Annual cycle

In South Africa, even seasonality shows fine-scale characteristics (see Fig. 3 and the Introduction) that RCM do not systematically capture. This section aims at investigating to what extent a current state-of-the-art RCM succeeds at simulating and regionalizing such spatially contrasted seasonality in South African rainfall.

For each station or grid-point, the relative contribution (in %) of each month to the total annual amount is first calculated, the wettest (driest) month being referred to as  $M_{\max}$  ( $M_{\min}$ ). The amplitude of the annual cycle is computed for each station or grid-point as the difference between these extreme values and is thus expressed in percentage points (pp).

Observations (Fig. 3) show the well-known maximum rainfall winter/summer timing opposition between the southwestern tip of Africa and the northeastern parts of the country. In addition, Fig. 3 also shows that the annual cycle has a weaker amplitude along the South Coast with roughly similar rainfall amounts all year round in agreement with Rouault and Richard (2003). Further north the inland parts of the Western Cape form a transition region between winter and summer rainfall. WRF captures rather well these features, in spite of some timing errors (Fig. 4). WRF generates most of its rain over Southern Africa in November and December whereas GPCP-1dd shows its annual rain peak mostly between January and March. The



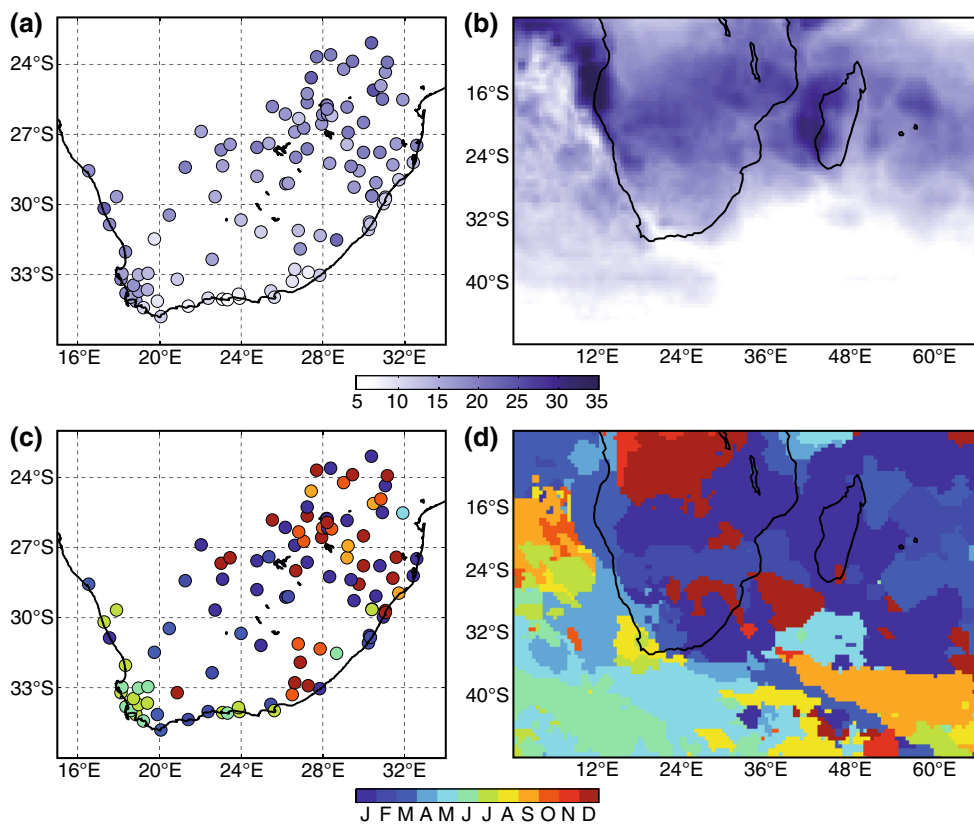


**Fig. 3** **a** Amplitude (pp) of the annual cycle according to rain-gauge records, 1998–2006. See text for details. **b** As **a** for GPCP-1dd. **c** Month associated with largest rainfall amounts ( $M_{\max}$ ) according to rain-gauge records. **d** As **c** for GPCP-1dd

situation is spatially contrasted at the scale of South Africa, with the rainfall peak occurring in January–March over the central parts of the country but slightly earlier in most of the stations located in the northeast (Rouault and Richard 2003). Rainfall derived from ERA-Interim presents a pattern almost identical to GPCP-1dd (not shown); this suggests that the minor timing errors identified in Figs. 3, 4 mostly result from errors internal to WRF (and not from its forcing boundary conditions).

Over South Africa, the amplitude of the annual cycle is under- (over-) estimated in BMJ (Grell) simulation, and appears as more realistic in KF and particularly KFtr. Errors are of larger magnitude at the domain scale, with a clear under- (over-) estimation of seasonality over the South Atlantic (the central Indian Ocean and the mid-latitudes). Over Africa results depend on the convective scheme used and are spatially noisy and contrasted, except for Grell that over-estimates seasonality over tropical Southern Africa, and KFtr that has similar errors but of smaller amplitude over equatorial Africa. All simulations succeed however in capturing adequately the seasonal locking of rainfall maximum as inferred by the wettest month of the year  $M_{\max}$  (as well as the driest month of the year  $M_{\min}$ , not shown), even if some local differences exist

between WRF simulations (Fig. 4) and GPCP-1dd (Fig. 3d). Over Africa they mostly consist in a tendency to simulate the annual rainfall peak too late over tropical Africa (January/February instead of December), and the other way around at subtropical latitudes. Given the relative shortness of the period analyzed (10 years) and the lack of ensemble simulations, it is however not possible to assess whether these discrepancies can be attributed to model deficiencies, sample size or to the internal variability of the system.

The annual cycle of precipitation in the four subdomains in South Africa (shown in Fig. 1) are presented in Fig. 5. We plot here values in  $\text{mm h}^{-1}$  in order to document both the timing and amplitude of the simulated annual cycle of simulated rainfall against observations. As a whole, the distribution of South African rainfall over the annual cycle is remarkably well reproduced by the model, whatever the regional index considered, albeit some important biases in the simulated amounts.

In the northeastern and northwestern parts of the country rainfall show a clear unimodal repartition with a peak in austral summer (November through March). Rainfall amounts are about three times larger in the Northeast than in the Northern Cape. Over these regions, WRF accurately

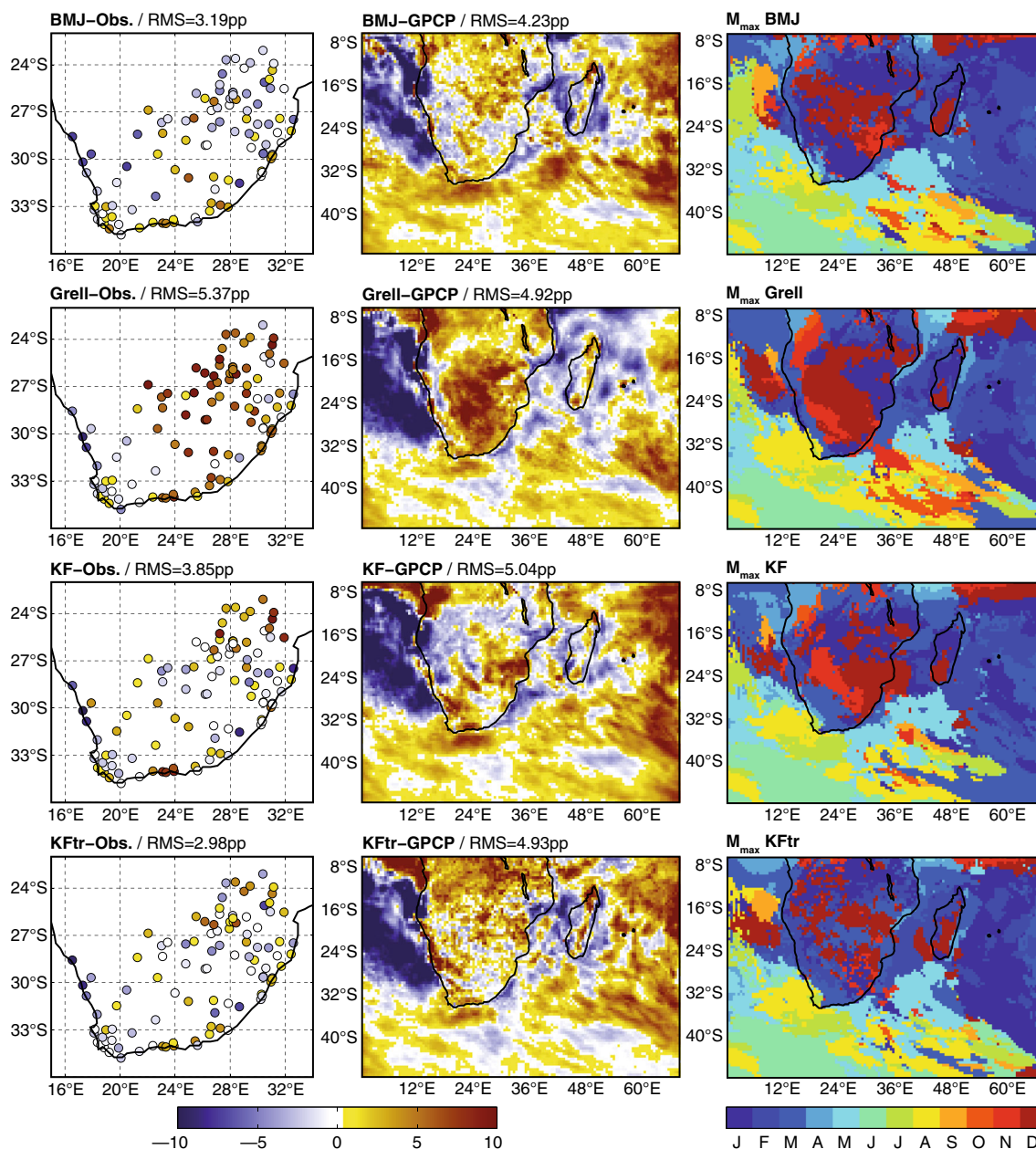
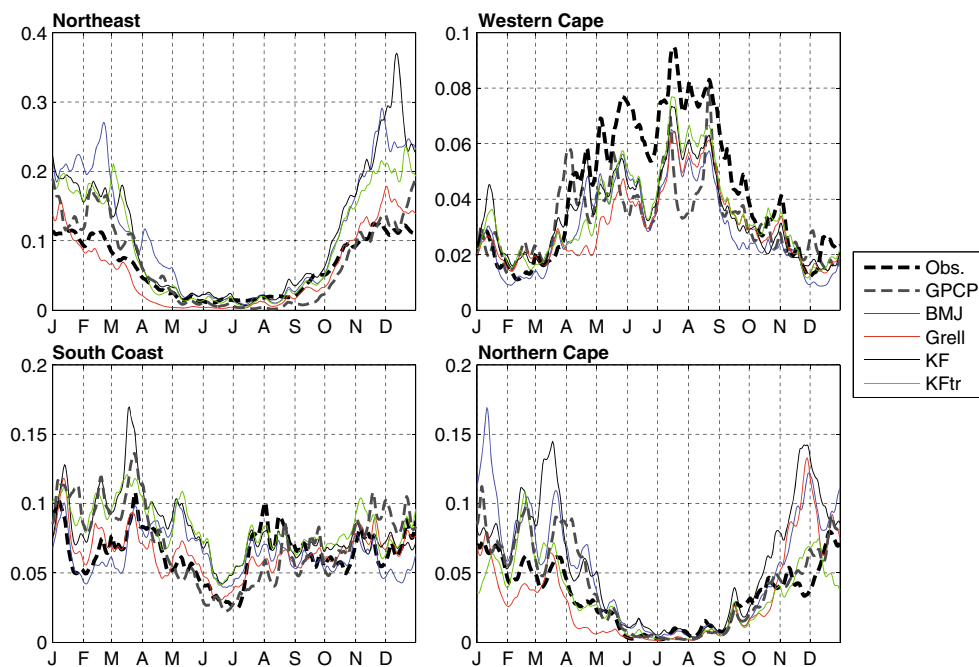


**Fig. 4** Left-hand column WRF-simulated biases in the amplitude of the annual cycle against rain-gauge records. RMS errors are labeled on the figure. Middle column the same against GPCP-1dd. Right-hand column  $M_{max}$  according to WRF simulations

simulates the austral summer rainfall peak, but with a clear overestimation reaching its maximum during the core of the rainy season. Rainfall overestimation is less important against GPCP-1dd, sensibly wetter than rain-gauge records between late December and April–May. KFtr and Grell experiments produce less biased results. Better results are also obtained during the dry (austral winter) season for those summer rainfall regions for all convective schemes. Figure 5 shows thus that the annual mean biases over these regions, as shown in Fig. 2, occur mostly in summer (i.e., the wet) season.

In the Western Cape region, the main rainfall peak occurs between April and August. WRF successfully simulates seasonality over the southwestern tip of Africa. Simulated rainfall amounts there are also realistic, in spite of a slight underestimation of seasonal amounts during the wet (i.e., winter) season against rain-gauge records. GPCP-1dd provides however rainfall amounts that are almost identical to those simulated. Results are not sensitive to the convective scheme used. This good performance of the model could be due to the lower contribution of convective rainfall there at this time of the

**Fig. 5** Average annual cycle of rainfall ( $\text{mm h}^{-1}$ ) in the four regions defined in Fig. 1. Results were 30-day lowpass filtered for readability



year (not shown), and the orography that characterizes the region.

As previously depicted in the literature (Rouault and Richard 2003), the regions of South Africa close to the South Coast show less marked seasonality, all months with similar rainfall amounts (Fig. 5). The driest months are June and early July. Once again, WRF produces convincing results, both in terms of annual distributions, timing, and simulated amounts. The model tends to produce too wet conditions between February and May, accurately reproduces the relative seasonal dryness in June, and produces fairly realistic results from August to December. Results are weakly physio-dependent, which could also be explained by the weak contribution of convective rainfall in this region during all seasons of the year (not shown): according to WRF the coastline forms a sharp limit separating the coastal regions (mostly dominated by stratiform rainfall) and the Agulhas current system, clearly enhancing convective activity locally.

To summarize, the model successfully simulates the annual cycle of rainfall over South Africa. Annual overestimations of rainfall are due to errors in simulated amounts that are clearly restricted to the core of the rainy seasons (winter in the southwestern part of the country, summer in most other parts).

### 3.3 Diurnal cycle

With a great variety of diurnal cycles (Rouault et al. 2013), its subtropical location that places the country under the influence of both tropical convection and mid-latitude

dynamics, and thanks to a dense network of hourly rain-gauge records, South Africa appears as an excellent place to investigate the diurnal cycle of rainfall at relatively fine scales, and how it can be simulated by an RCM.

Analyses are carried out over the austral summer (November through March) season, although the case of the austral winter season will be briefly mentioned below. The average diurnal cycle  $\bar{c}$  is first calculated over the whole period for each time series  $x$  (rain gauge record or WRF grid). The average contribution (in %) of each hour of the day to the total amounts is also computed. As for the annual cycle (Sect. 3.2), the amplitude of the diurnal cycle (in percentage points, pp) is defined as the difference between the largest and the lowest hourly contribution (resp. denoted  $H_{\max}$  and  $H_{\min}$ ). The variance explained  $V$  by the diurnal cycle (in %) is calculated as the ratio between the variance of the residuals to the average diurnal cycle and the raw time series:

$$V = \left( 1 - \frac{\text{var}(x - \bar{c})}{\text{var}(x)} \right) \times 100.$$

Figure 6 shows the amplitude of the observed and simulated diurnal cycles. In the observation, and in agreement with Rouault et al. (2013) using the same rainfall dataset, largest amplitudes are in the eastern and northeastern parts of the country, i.e., the region most submitted to convection (either due to tropical influence in the north, or to orographic lifting over the Drakensberg mountains in the east: Tyson and Preston-White 2000; Blamey and Reason 2013). This is also where rainfall amounts are largest on average (Fig. 2), especially during the austral summer season



**Fig. 6** Amplitude of the diurnal cycle **a** for each rain gauge station; **b** each WRF grid point, and **c** biases (pp) for each WRF grid containing at least one station (*lower panels*). RMS errors are labeled on the figure

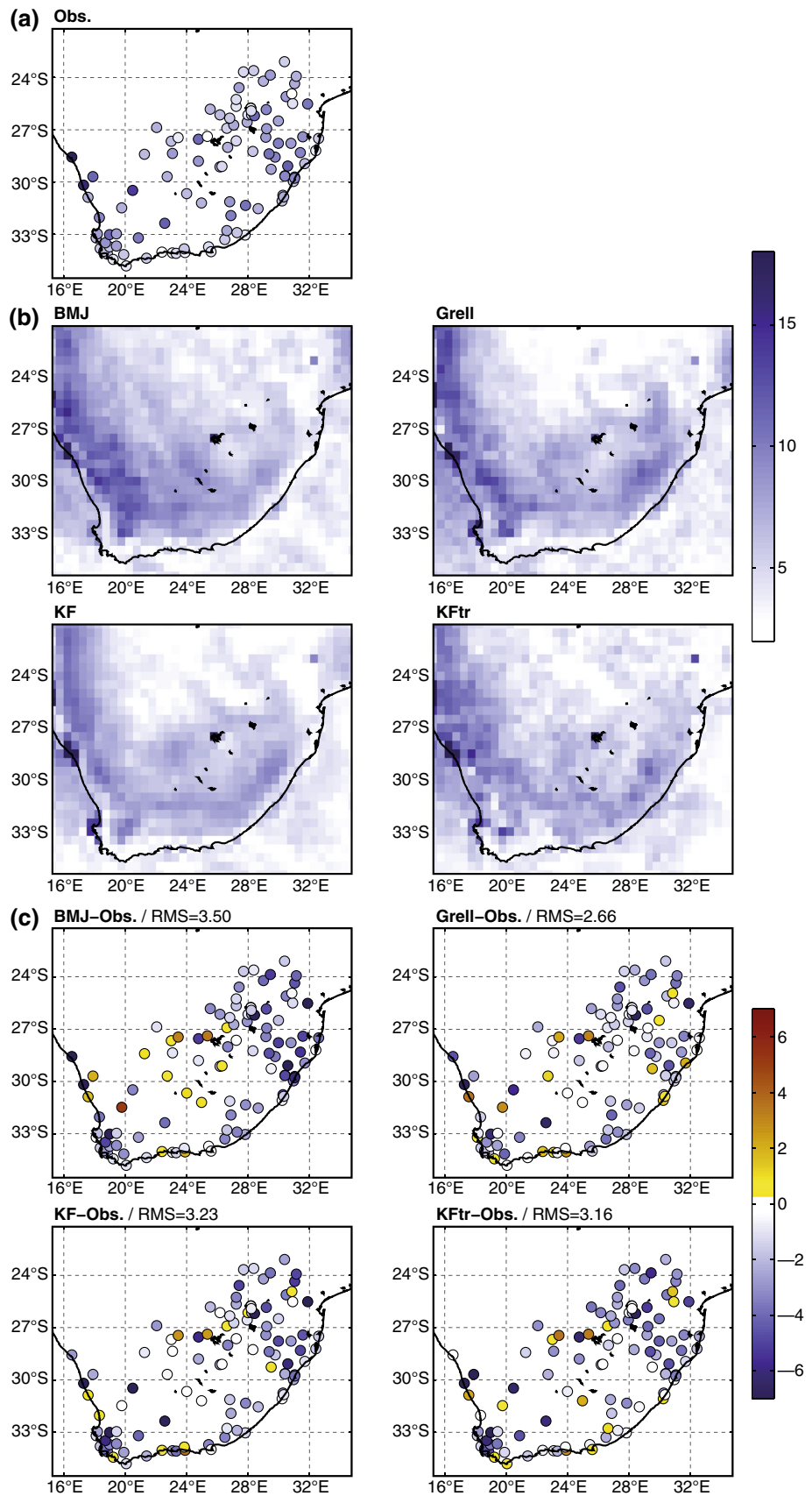
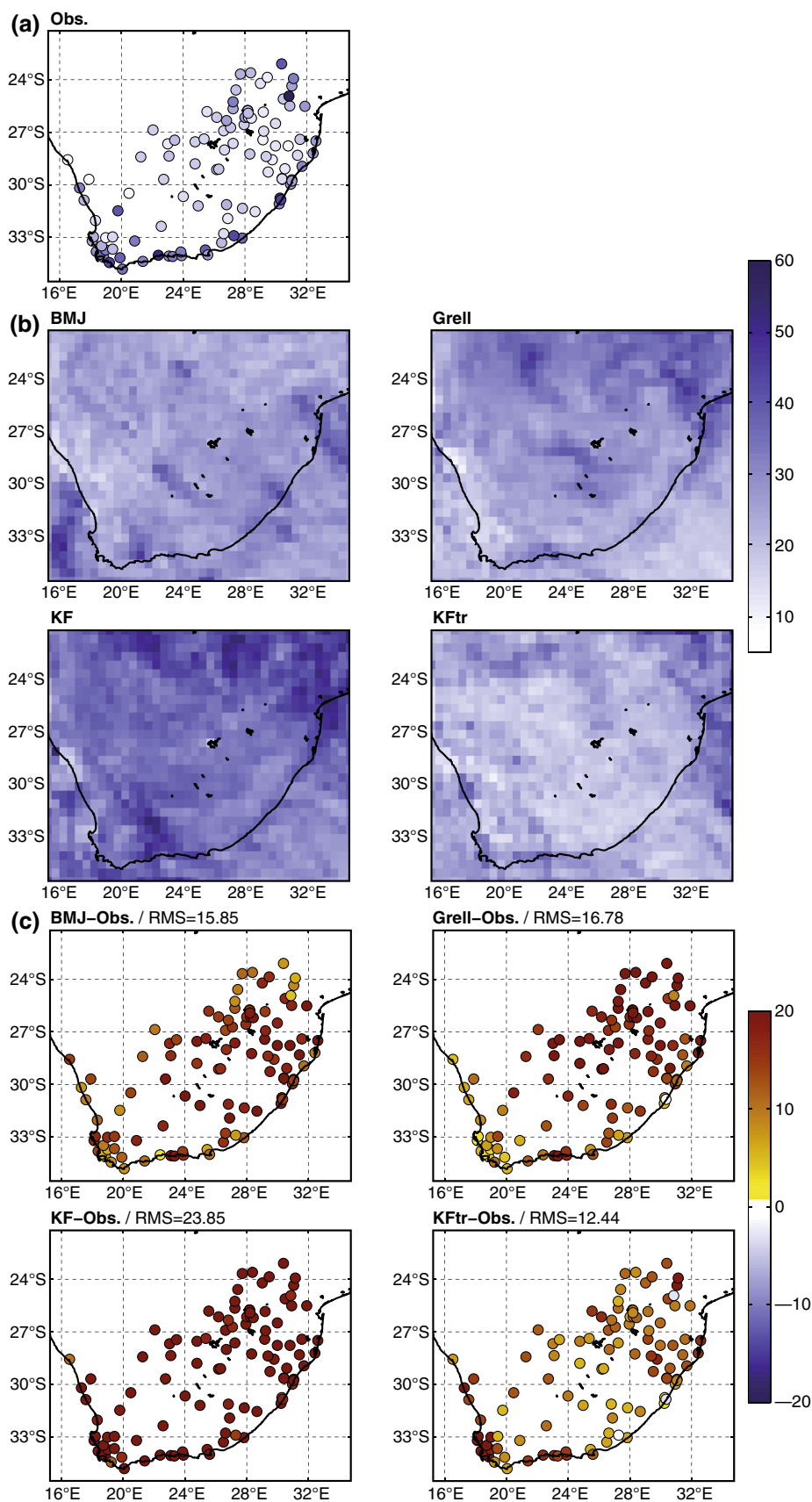


**Fig. 7** As Fig. 6 but for the variance explained (%) by the diurnal cycle. See text for details

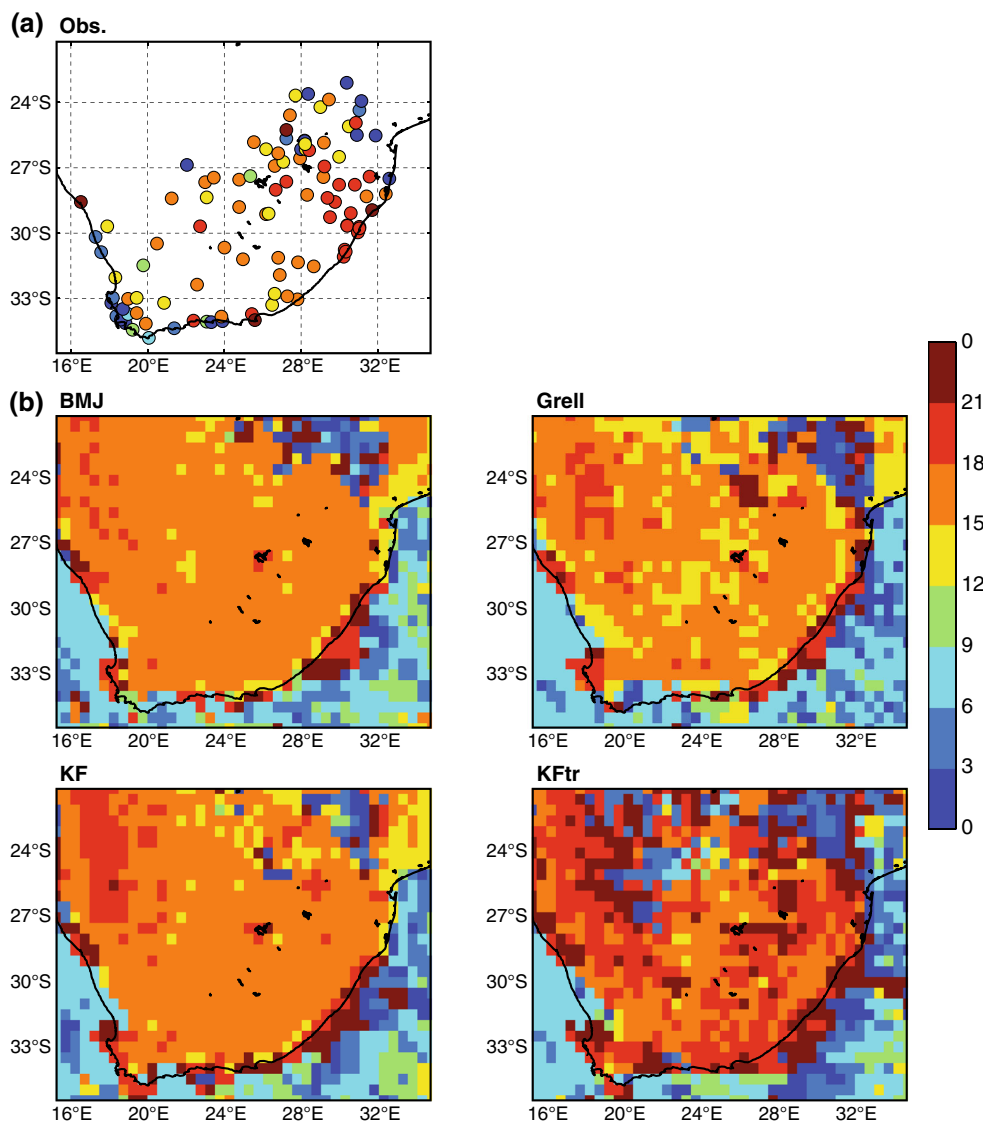


(Figs. 3, 4, 5). In contrast, amplitudes are quite weak in the Western Cape, experiencing its dry season at this time of the year (Fig. 5).

WRF shows a tendency to slightly under-estimate diurnal amplitudes (Fig. 6). They are largest near the Drakensberg mountains in the Eastern Cape and KwaZulu-Natal provinces, especially in the Grell experiment, and also, more surprisingly, over the Northern Cape region in the northwestern part of the country. There, stations are too few to assess properly the quality of the simulated diurnal cycle and its regionalization. Further north diurnal amplitudes tend also to decrease, which cannot be confirmed in the absence of observation. Largest negative biases are in the northeastern parts of South Africa. The South Coast and the Western Cape also tend to show weak but yet significant underestimations of diurnal amplitudes. The centre of the country shows weak positive biases.

The variance explained by the diurnal cycle (Fig. 7) is rather large (typically, 20–40 %) and homogeneous spatially over South Africa in the observation. It is generally larger (weaker) near the coasts (in the hinterland). WRF produces less convincing spatial patterns and clearly overestimates the variance associated with the diurnal cycle. Results also appear to be strongly physic-dependent (Fig. 7b). BMJ and Grell are in good agreement, KF producing the largest values while the same scheme used with an alternative trigger function simulates a diurnal cycle responsible for the smallest fraction of the overall variance. Given that WRF generally overestimates the variance explained by the diurnal cycle, the best (worst) results are thus obtained with KFtr (KF) scheme. These results illustrate the importance of the trigger function for the diurnal cycle, even if simulated amplitudes are almost identical (Fig. 6).

**Fig. 8** Phasing of the diurnal cycle: hour of the day associated with the largest rainfall amounts for each rain gauge station (a) and WRF grid point (b)



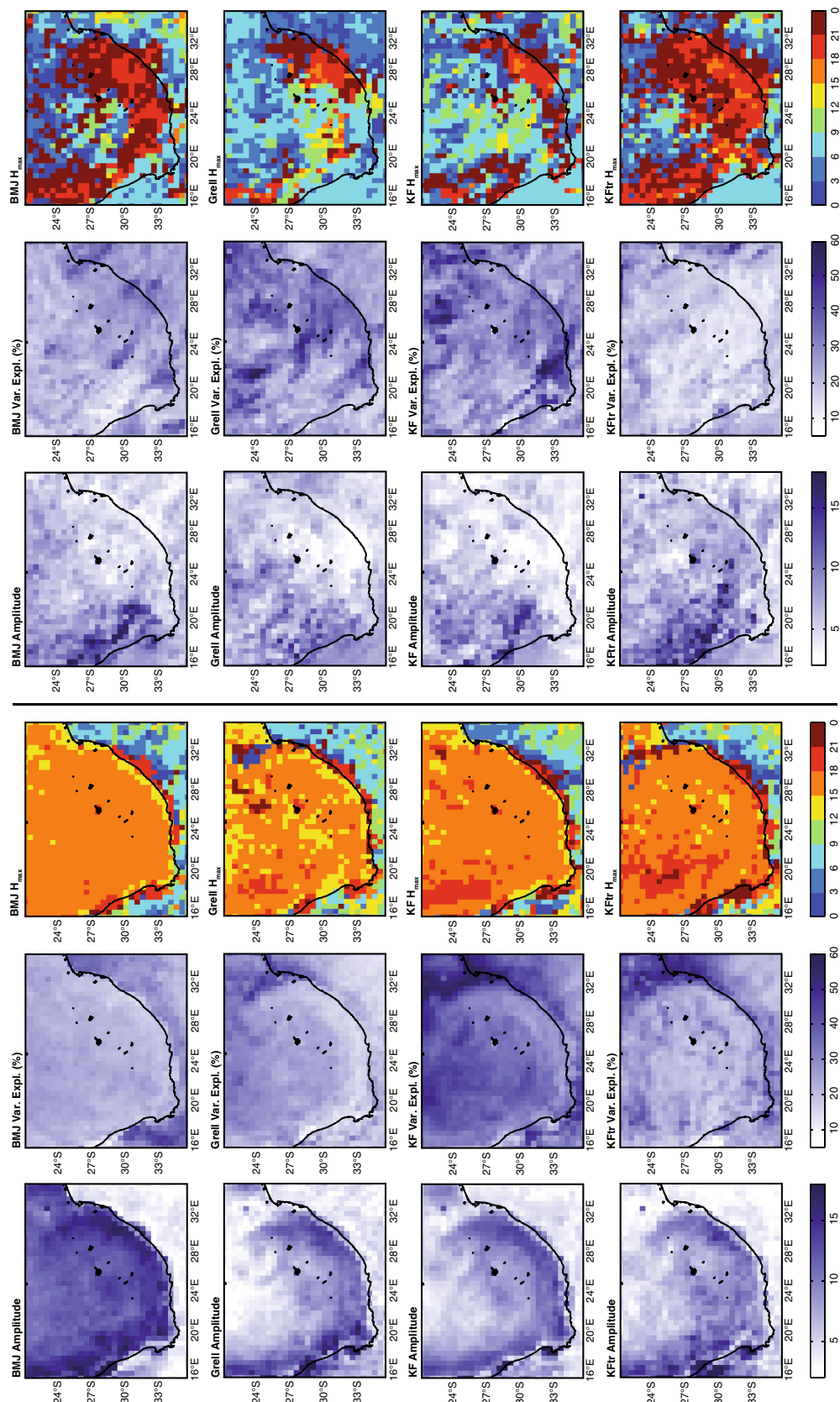


**Fig. 9** Amplitude, explained variance and  $H_{\max}$  for convective (left-hand panels) and stratiform (right-hand panels) rainfall simulated by each WRF experiments (in rows)



**Fig. 10** Average diurnal cycle of rainfall ( $\text{mm h}^{-1}$ ) in the four regions defined in Fig. 1 **a** for the austral summer season (November through March); **b** for the austral winter season (May through July)

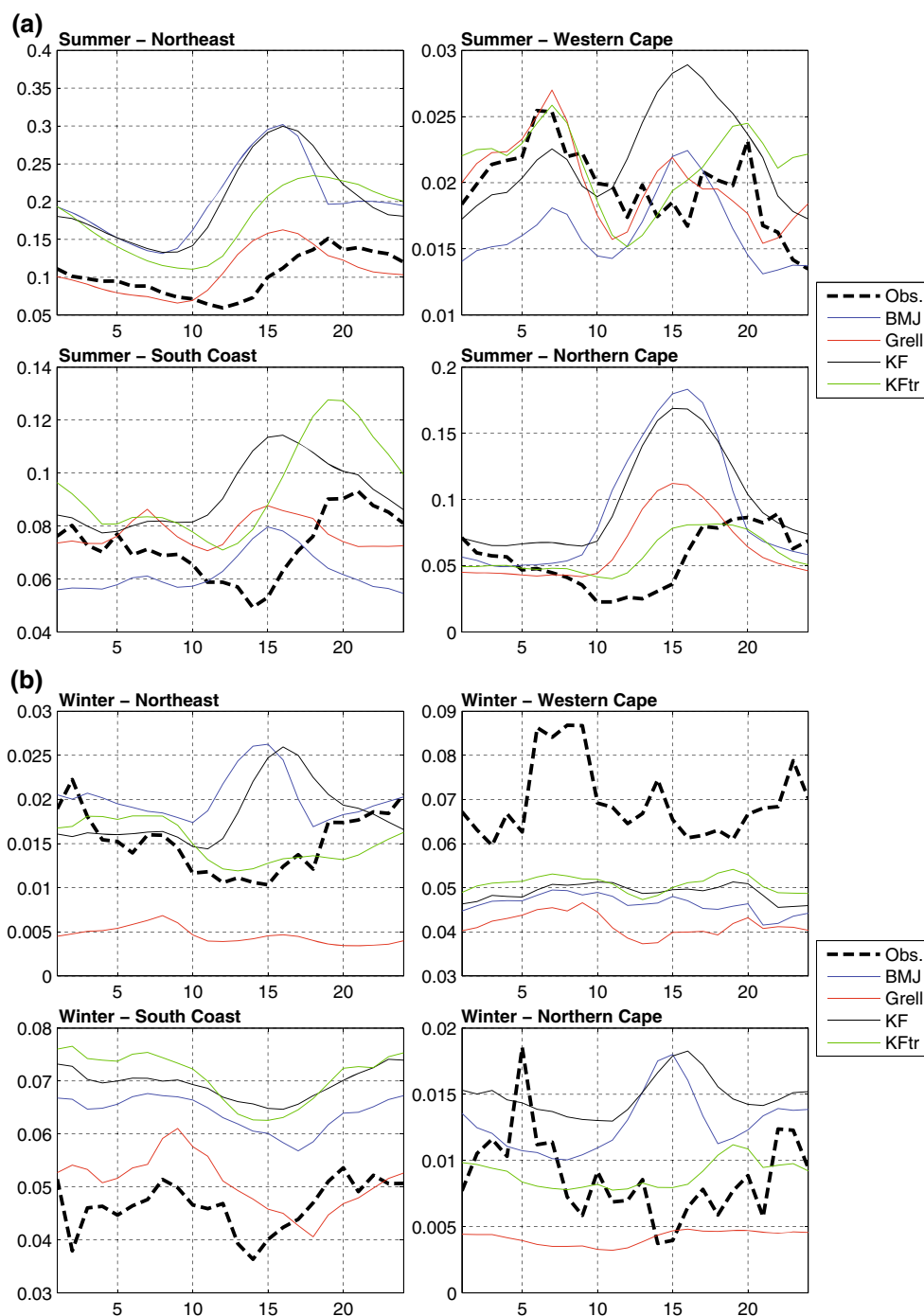


Figure 8 shows the timing of the diurnal cycle, as inferred by the hour of the day  $H_{\text{max}}$  associated with the largest observed and simulated rainfall amounts. Confirming once again Rouault et al. (2013), the rainfall peak occurs in the early evening or nocturnal hours over most regions (including the South and West coasts). The stations experiencing rainfall in the early hours of the afternoon (such as found in most tropical regions where convective rainfall is predominant) are quite rare.

The simulated rainfall peak occurs roughly 2–3 h too early over the continent (Fig. 8b). Previous works already noted a tendency for most convective schemes to produce rainfall peaks in the early afternoon (e.g., Nikulin et al. 2012). Further north over Zimbabwe, there is a nocturnal peak in rainfall, but due to lack of observed data there does not allow us to assess its validity. Over nearby oceans, largest rainfall amounts are simulated during the early hours of the morning (or between 21 h and midnight over

parts of the Agulhas current). BMJ, Grell and KF produce quite convergent results, but the trigger function used in KFtr once again contributes to a later rainfall peak producing more realistic results. Reasons for this improvement are investigated below.

Separating the convective and stratiform components of simulated rainfall provides new insights that were concealed when analyzing total rainfall as a whole (Fig. 9).

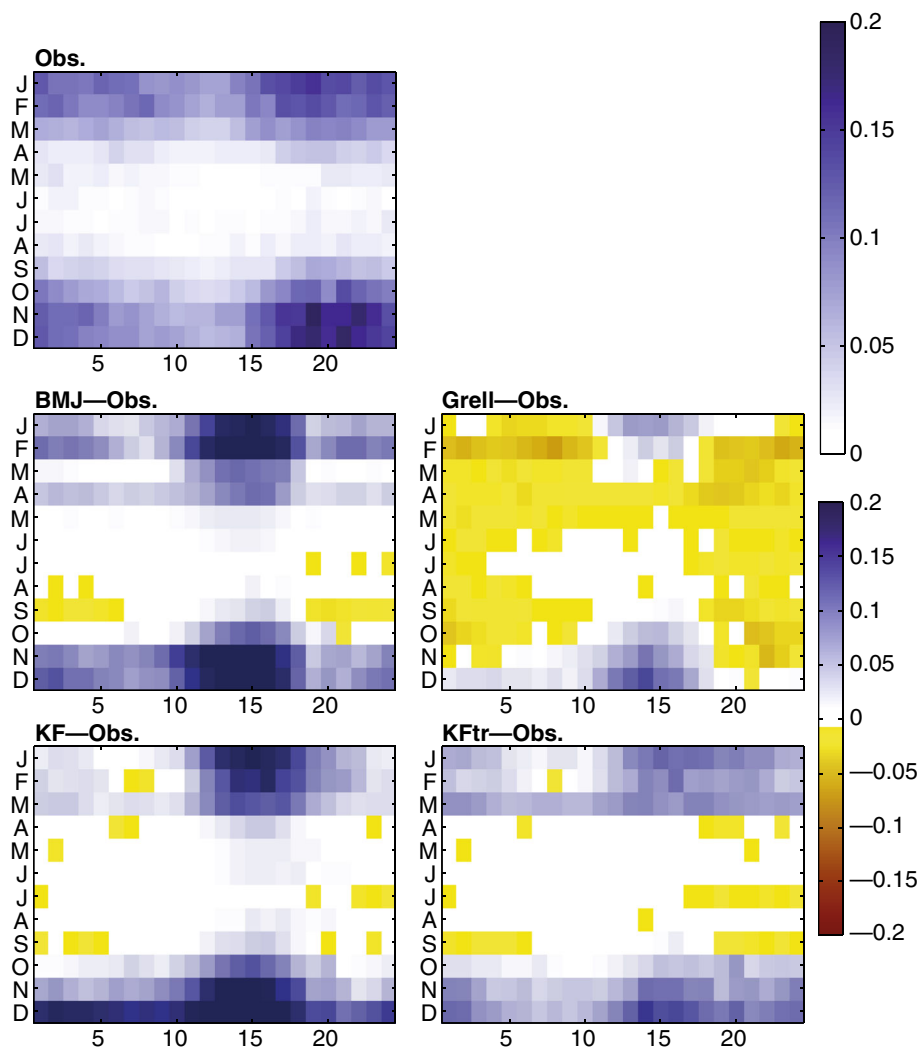
- All schemes simulate a peak of convective rainfall in the late afternoon. Peaks of stratiform rainfall occur at night. The apparent better results produced by KFtr in terms of phasing are thus mostly due to a larger contribution of stratiform rainfall over South Africa (Table 1) rather than a delayed initiation of simulated convection.
- The timing and amplitude of stratiform rainfall differ sensibly from one experiment to another. This illustrates once more how the convective parameterizations deeply interact with cloud microphysics responsible for

the rain-bearing systems explicitly simulated by the model. They indirectly impact stratiform rainfall by modifying atmospheric instability, and the amounts of precipitable water left in the air column.

- BMJ convective rainfall fraction shows a clear land-sea contrast, with large diurnal amplitudes over the continent explaining a moderate fraction of the overall rainfall variance. BMJ actually produces virtually no convective rainfall over the continent at night (between 21 and 7 h, not shown). This is not so clear for other schemes.

Results concerning the diurnal cycle are extended to the austral winter season in Fig. 10 for the four regional indices shown in Fig. 1. During the summer season previously discussed, all convective schemes produce too early and too abundant rainfall peaks in the afternoon in the northern parts of the country influenced by tropical convection. Grell simulates the most realistic amounts, confirming Cr  tat et al. (2012). KFtr simulates a peak later in the

**Fig. 11** Intersection between the average diurnal and annual cycles of rainfall ( $\text{mm h}^{-1}$ ) in the northeastern index shown in Fig. 1 for observation, and biases of the four WRF simulations against observations



afternoon, mostly due to lower convective rainfall amounts. The Western Cape experiences dry conditions during summer. Along the South Coast, observations also show a rainfall peak occurring during the early hours of the night, which all WRF simulations (except KFtr) fail at reproducing.

During the winter season, the Western Cape tends to show a rainfall peak in the early hours of the day. All simulations underestimate rainfall amounts and show a completely flat diurnal cycle. The South Coast presents a complex cycle, with increased (decreased) rainfall in the morning and in the night (in the afternoon) that the model reproduces quite well. Northern regions are drier during this season and show no clear diurnal cycles. As for the rainfall in the Western Cape, the amplitude of the observed diurnal cycle and variance of the diurnal cycle is weak.

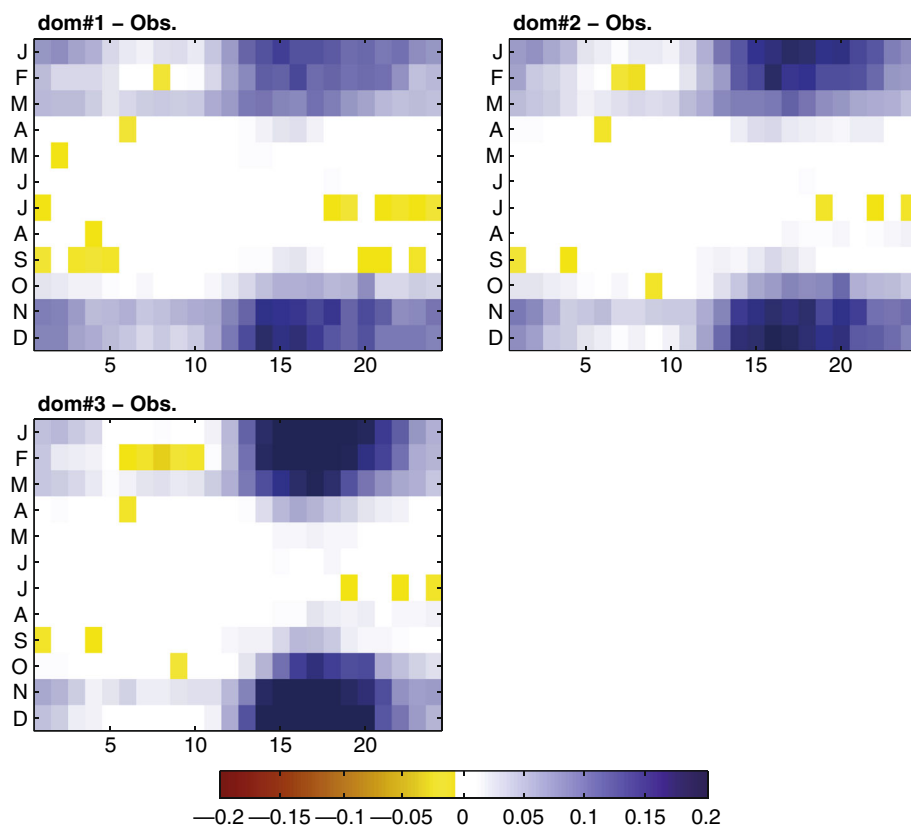
Taken together, Figs. 5 and 10 allow further investigations of the model average biases shown in Fig. 2b and already reported in previous studies (Cr  tat et al. 2011, 2012; Ratnam et al. 2012; Vigaud et al. 2012; Ratna et al. 2013). In addition, and as an example using the Northeast domain only, Fig. 11 shows the season and the hour of the day at which largest errors are concentrated.

The Western Cape and the South Coast show fairly realistic simulated amounts on average (Figs. 5, 10). There is a weak underestimation of the main winter rainfall and

an even weaker overestimation of austral fall rainfall along the South Coast from February to June. These biases in the Western Cape and the South Coast are almost equally stratified over the diurnal cycle (Fig. 10).

In the northern parts of South Africa, as well as the east coast of the Eastern Cape and KwaZulu-Natal, convection has a greater importance. There, annual rainfall is strongly overestimated (Fig. 2) but these errors are by far largest during the wet (summer) season (Fig. 5). Close examination of the diurnal cycle simulated in austral summer shows that it is the convective peak of early afternoon that accounts for a major part of such errors, its magnitude being approximately two times too large in both region (in addition to its perfectible timing, Fig. 10). Rainfall amounts during other hours of the day (especially during the night) are in contrast rather close to observed ones. Figure 11 shows the physic-dependency of these results over the northeastern regional index. The realistic rainfall amounts obtained with Grell convection in summer correspond actually to weak wet afternoon biases counter-balanced by dry biases during some hours of the night and the morning. During the dry season (April through September) dry biases are generalized. Summertime wet biases are largest for other convection schemes, a few hours before the observed rainfall peak occurring during the first half of the night. They are more diffuse temporally in KFtr

**Fig. 12** As Fig. 11 but for the biases of the three nested domains of the N3 experiment



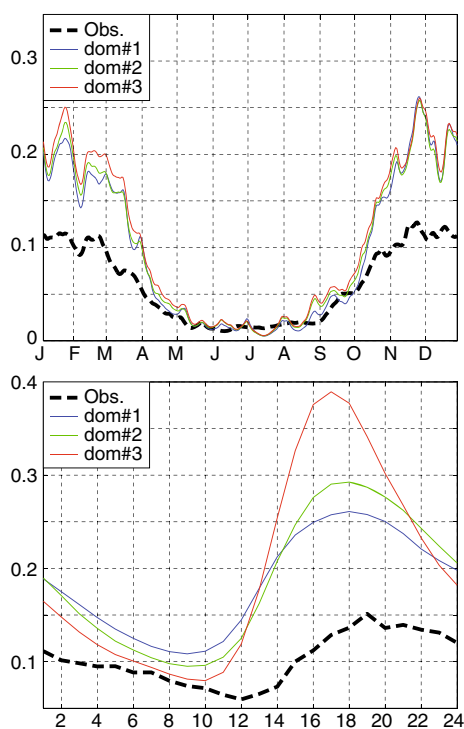


**Fig. 13** Average seasonal (*upper panel*) and diurnal (*lower panel*, for the November through March season) cycles of rainfall ( $\text{mm h}^{-1}$ ) in the northeastern regional index, for the three nested domains of N3 experiment

experiment compared to KF and BMJ, confirming its more realistic phasing with observations. During the dry season biases are close to zero.

### 3.4 Sensitivity to the model resolution and cloud-resolving simulations

Largest biases being due to a deficient simulation of convective rainfall (Sect. 3.3), this section uses an additional experiment performed at a considerably finer resolution over the same period, described in detail in Sect. 2. We analyze here mainly domains #2 and #3 (resp. set at roughly 18.3 and 3.6 km), with domain #3 resolving atmospheric convection explicitly over the northeastern regional index (Fig. 1). We choose this region because it is the wettest region of South Africa (Fig. 2) and also because it is under the largest influence of deep tropical convection, especially during the austral summer rainy season (Tyson and Preston-White 2000).

Figure 12 first shows that the biases found for KFtr exp. are not dramatically reduced when the spatial resolution is increased (domain #2) or when atmospheric convection is resolved (domain #3). This result differs from Marsham et al. (2013) who radically improved the representation of the simulated diurnal cycle of atmospheric convection over West Africa using an explicit representation of convective

cells. Figure 13 even shows that the diurnal cycle of rainfall is more poorly reproduced in domains #2 and #3 compared to domain #1. Noteworthy here is an increase in the amplitude of the diurnal cycle and a tendency to produce the diurnal maximum (minimum) of rainfall slightly earlier (later), leading thus to a sharper increase in the simulated amounts between the late hours of the morning and the afternoon. As already suggested in Fig. 12, overall amounts tend also to be larger and therefore result in increased wet biases. This is due to a much more pronounced rainfall peak in the afternoon that is not counter-balanced by the slightly drier conditions simulated during the night and the morning.

Seasonally, these differences between the three nested domains are largest between January and March, the second half of the summer rainy season, while they are close to zero during the other months, even in the first half of the rainy period (including October, November and December). Such differences between the early and late parts of the summer rainy season are reminiscent of D'Abreton and Lindesay (1993) and D'Abreton and Tyson (1995), who depict a predominant importance of zonal fluxes and transient variability in October (early summer), but more important meridional fluxes embedded in the seasonal mean circulation in January (late summer). Additional analyses are required to understand whether these differences in the observed mean climate can impact simulated rainfall amounts (especially in terms of seasonal and diurnal cycles), but are beyond the scope of the present study.

At the local (grid-point) scale, Fig. 14 shows how the basic features of the diurnal cycle (i.e., amplitude, variance explained and timing) vary from one domain to another, i.e., how they can be downscaled and to what extent they are sensitive to the model resolution. Of course, local information is gradually gained from domain #1 to #3, even if there is a general agreement between the nested and the parent domains. For instance, according to domain #1, the amplitude of the diurnal cycle is largest along a NW–SE band linking Swaziland to Botswana and crossing South Africa between Pretoria and Pietersburg. Domains #2–3 confirm and detail this pattern (Fig. 14). For domain #3, more realistic surface conditions also help to identify more localized features of the diurnal cycle. For instance (1) orographic effects are clearly better simulated, especially east of Pietersburg where terrain elevation rapidly decreases. This results in a weaker amplitude of the annual cycle there, which explains however a larger fraction of the variance compared to the nearby Drakensberg massif further west; (2) land-use categories also lead to more contrasted features of the diurnal cycle locally. One can note indeed particularly strong amplitudes over a moderate-sized water body, Vaal Dam Reservoir, roughly 75 km



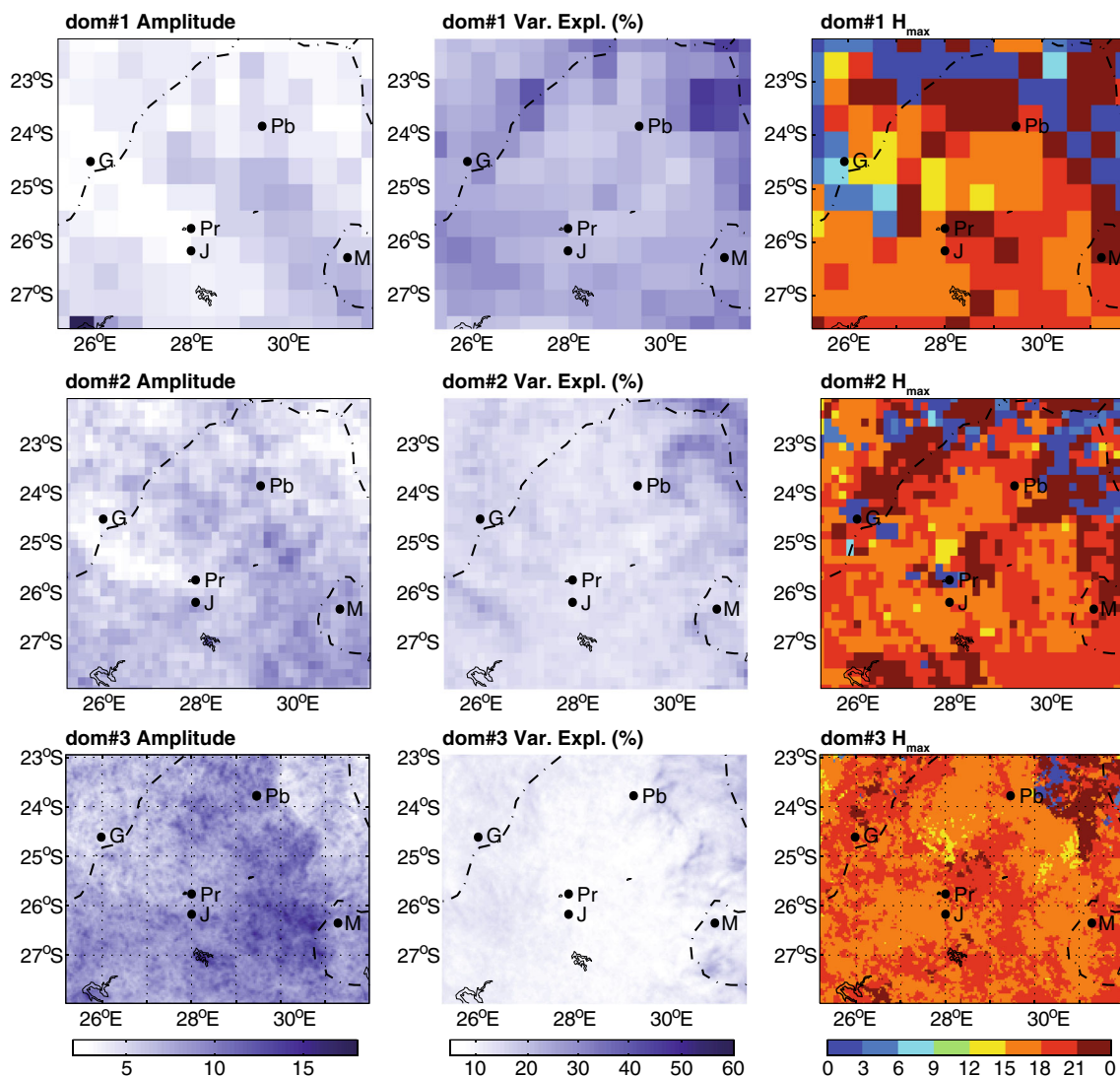


**Fig. 14** Amplitude, explained variance and  $H_{max}$  over the northeastern regional index for the three nested domains of N3 experiment. The dashed lines show political boundaries and the points the main

cities of the area: Johannesburg (J), Pretoria (Pr) and Pietersburg (Pb) in South Africa, Gaborone (G) in Botswana, and Mbabane (M) in Swaziland

south of Johannesburg. More generally, increasing the model resolution, and ultimately using cloud-resolving simulations, leads to (1) generally increased amplitudes (reducing thus the biases noted in Fig. 6 compared to rain-gauge data points); (2) reduced explained variance (improving once again the results discussed in Fig. 7); (3) more contrasted results concerning the timing of  $H_{max}$  but with a tendency to simulate heavy rainfall earlier in the afternoon. These differences in the phasing of the diurnal cycle, already shown in Figs. 12, 13 at the scale of the northeastern regional index, do not clearly contribute to improve the timing, such as revealed by data points (Fig. 8). As for the parent domains and other WRF simulations, observed and simulated diurnal cycles are roughly shifted by  $\sim 2$  h (Figs. 10a, 13), rainfall (and more

particularly convective rainfall) occurring too early in the model (Fig. 9) as in most previous studies (see the Sect. 1).

Figures 12, 13 and 14 give thus contrasting pictures of the improvements and modifications of the simulated diurnal cycle produced by the increased resolution and the explicit convection. On the one hand, the basic properties of the diurnal cycle are clearly improved in WRF nested domains (except for its phasing). However, over West Africa, Marsham et al. (2013) obtained a more realistic phasing of their diurnal cycle in their cloud-resolving simulation, although their parameterized simulation was more biased than our first series of four simulations discussed in Sect. 3.3. On the other hand, simulated rainfall amounts are larger than in domain #1, hence increased wet biases, especially during the austral summer rainy season

and in the afternoon (Fig. 12). In the end, the main deficiencies of the model consist in these large, persisting wet biases over the northern (tropical) part of South Africa, while the diurnal and seasonal distributions of simulated amounts can be considered as reasonably well reproduced, in spite of perfectible phasing of the late afternoon rainfall peak.

The rather large size (roughly  $752 \times 570$  km) of cloud-resolving domain #3 ensures that spatial high frequencies discussed above are properly resolved by the model, without too strong interferences with lateral forcings that would prevent the model to develop small-scale features (Leduc and Laprise 2009). Yet, even for domain#3, the physic-dependency of our results (especially the lack of reduction of the model biases) and the sensitivity to lateral boundary conditions provided by the parent domains (using parameterized convection) need to be tested in future work.

#### 4 Conclusion and discussion

While most RCM-based studies on Southern Africa used the seasonal scale so far, the aim of this work is to illustrate how a current state-of-the-art RCM reproduces the diurnal and annual cycles of rainfall over the region, both known to present some spatially contrasted specificities (e.g., Tyson and Preston-White 2000; Rouault et al. 2013). Regional experiments are performed using the non-hydrostatic WRF model, simulating hourly rainfall over the 1998–2006 period using four alternative parameterizations for deep atmospheric convection. A fifth simulation resolves convection explicitly over northeastern South Africa. Model outputs are compared to a network of 103 rain-gauge stations, available over the same period and at the same hourly timescale, and covering the whole South African country. Results can be summarized as follows.

- In agreement with previous studies (Crétat et al. 2012; Ratna et al. 2013), the model mean biases are strongly dependent on the convective scheme used in the simulation. The Kain–Fritsch scheme clearly produces the largest rainfall overestimation, while the Grell–Dévényi scheme tends to produce slightly too dry conditions. This corroborates Ratna et al. (2013), who explained KF scheme wet biases by too unstable atmospheric conditions and too large moisture convergence over the region, mostly advected from the tropics; Grell biases were in contrast imputed to opposite sign biases in moisture and instability, as inferred for instance by CAPE or vertical velocity in the free troposphere. The Betts–Miller–Janjic scheme provides rather realistic rainfall amounts. An interesting outcome of this work concerns the influence of the

convective scheme trigger function, investigated through the KFtr experiment using the moisture-advection based trigger developed by Ma and Tan (2009) in the Kain–Fritsch scheme. The use of this alternative trigger greatly reduces the wet biases discussed above. Additional analyses (not shown) also confirmed that the number of rainy days ( $>1 \text{ mm day}^{-1}$ ) is decreased, improving the performance of this scheme for simulating daily rainfall.

- Rainfall seasonality is well simulated over all parts of South Africa—including the Western Cape where winter rainfall dominates, the South Coast wet all months of the year, and the northern parts of the country where summer rainfall is prevalent. Average rainfall biases are not stationary with time and are, as expected, sensibly larger in magnitude over the northern part of the country and during the austral summer rainy season, when convection is intense over the continent. Rainfall biases are more constant over the Western Cape region, experiencing dominant, mostly stratiform, winter rainfall.
- The timing of the diurnal cycle is shifted by  $\sim 2\text{--}3$  h against observations, the rainfall peak occurring during the first half of the night over most regions inland being simulated during the late afternoon in WRF simulations. KFtr experiment provides slightly better results, mainly due to a larger contribution of stratiform rainfall to the total rainfall amounts while convection still peaks in the afternoon. All convective schemes strongly overestimate rainfall during the afternoon hours of the rainy season, while moderate biases prevail during the morning hours, as well as during the other months of the year. The average model biases found at the annual/climatological scales are thus mostly imputable to the periods during which atmospheric convective activity is most active.
- The cloud-resolving experiment simulates increased wet biases over the South African hinterlands, especially during the second half of the summer rainy season; the timing of the diurnal cycle is not dramatically improved but its amplitude and the fraction of variance explained are closer to observations.

These results are useful to better understand the causes of the model biases over the region. The sensible improvement due to the use of the moisture-advection based trigger function in the KF convective scheme confirms that the onset criterion for atmospheric convection in the model is a key parameter strongly impacting both its steady state and its simulated diurnal cycle (Dai et al. 1999; Dai and Trenberth 2004).

Another interesting issue comes from the comparison between parameterized and explicit convection. The better

results obtained with the cloud-resolving simulation could either be due to a “resolution effect”, reducing the statistical bias due to the point-to-grid comparison between rain-gauge records and model outputs, or to more realistic simulation of rain-bearing systems, including their convective component, and made possible by the lack of parameterizations. Yet, even in a cloud-resolving model over a region dominated by convective rainfall, simulated amounts present large rainfall overestimations. This suggests that such biases could be produced by the parameterizations of cloud microphysics or radiative transfers. Over Equatorial Africa, Pohl et al. (2011) found indeed that shortwave radiation schemes induce uncertainties in the simulated climate that are at least of the same magnitude as those associated with convective schemes. Of course, the biases noted here could also result of complex and non-linear interactions between these families of parameterizations, or interactions between simulated stratiform and convective clouds. The results presented here nonetheless illustrate that working on the improvement of convective schemes alone will probably not bring all answers nor solve all problems, even in the tropics where convection is of primary importance.

As for Evans and Westra (2012) over eastern Australia, process-based studies are now needed to document the triggering mechanisms for convective activity (and more generally the diurnal cycle) over South Africa. Over eastern Australia in summer, atmospheric instability (CAPE), thermal convection and large-scale moisture convergence appear as the main rain-producing mechanisms. In South Africa, one could intuitively expect various influences from the triggering mechanisms as an explanatory key of the spatially contrasted features of both seasonal and diurnal cycles. A predominant role of atmospheric instability could be expected in the northeast, with a possible influence of thermal convection in the northwest. Over the Drakensberg and its eastern slopes topographic lifting could prevail, while frontal systems are probably the major triggering mechanism for rainfall occurring further south in the mid-latitudes and along the coast. The role of land and sea breezes convergence along with the influence of the warm Agulhas Current along the South Coast need to be examined in further detail. Given its rather good skill for simulating the diurnal and seasonal distribution of convection, WRF could be used to explore the respective influence of such mechanisms at relatively fine scales over the region in future studies.

**Acknowledgments** This work is a contribution to the LEFE/IDAO VOASSI programme funded by CNRS. The South African Weather Service provided the rainfall data. WRF was provided by the University Corporation for Atmospheric Research website ([http://www.mmm.ucar.edu/wrf/users/download/get\\_source.html](http://www.mmm.ucar.edu/wrf/users/download/get_source.html)). ERA-Interim data were provided by the ECMWF Meteorological Archival and

Retrieval System (MARS). Two anonymous reviewers helped improve the manuscript. Mathieu Rouault thanks NRF, WRC, ACCESS, Nansen-Tutu Center for funding and SAWS for rainfall data. Calculations were performed using HPC resources from DSI-CCUB, universit  de Bourgogne.

## References

- Betts AK (1986) A new convective adjustment scheme. Part I: observational and theoretical basis. *Q J R Meteorol Soc* 112:677–691
- Betts AK, Jakob C (2002) Evaluation of the diurnal cycle of precipitation, surface thermodynamics, and surface fluxes in the ECMWF model using LBA data. *J Geophys Res* 107(D20):8045. doi:10.1029/2001JD000427
- Betts AK, Miller MJ (1986) A new convective adjustment scheme. Part II: single column tests using GATE wave, BOMEX, ATEX and arctic air-mass data sets. *Q J R Meteorol Soc* 112:693–709
- Blamey RC, Reason CJC (2013) The role of mesoscale convective complexes in Southern Africa summer rainfall. *J Clim* 26:1654–1668. doi:10.1175/JCLI-D-12-00239.1
- Boulard D, Pohl B, Cr tat J, Vigaud N (2013) Downscaling large-scale climate variability using a regional climate model: the case of ENSO over Southern Africa. *Clim Dyn* 40:1141–1168. doi:10.1007/s00382-012-1400-6
- Chen F, Dudhia J (2001a) Coupling an advanced land-surface/hydrology model with the Penn State/NCAR MM5 modeling system. Part I: model description and implementation. *Mon Weather Rev* 129:569–585
- Chen F, Dudhia J (2001b) Coupling an advanced land-surface/hydrology model with the Penn State/NCAR MM5 modeling system. Part II: model validation. *Mon Weather Rev* 129:587–604
- Cook KH (2000) The South Indian convergence zone and interannual rainfall variability over Southern Africa. *J Clim* 13:3789–3804
- Cr tat J, Pohl B (2012) How physical parameterizations can modulate internal variability in a regional climate model. *J Atmos Sci* 69:714–724. doi:10.1175/JAS-D-11-0109.1
- Cr tat J, Macron C, Pohl B, Richard Y (2011) Quantifying internal variability in a regional climate model: a case study for Southern Africa. *Clim Dyn* 37:1335–1356. doi:10.1007/s00382-011-1021-5
- Cr tat J, Pohl B, Richard Y, Drobinski P (2012) Uncertainties in simulating regional climate of Southern Africa: sensitivity to physical parameterizations using WRF. *Clim Dyn* 38:613–634. doi:10.1007/s00382-011-1055-8
- D’Abreton PC, Tyson PD (1995) Divergent and non-divergent water vapour transport over southern Africa during wet and dry conditions. *Meteor Atmos Phys* 55:47–59
- D’Abreton PC, Lindsay JA (1993) Water vapour transport over southern Africa during wet and dry early and late summer months. *Int J Climatol* 13:151–170
- Dai A, Trenberth KE (2004) The diurnal cycle and its depiction in the community climate system model. *J Clim* 17:930–951
- Dai A, Giorgi F, Trenberth KE (1999) Observed and model-simulated diurnal cycles of precipitation over the contiguous United States. *J Geophys Res* 104(D6):6377–6402
- Dee DP, Uppala SM, Simmons AJ, Berrisford P, Poli P, Kobayashi S, Andrae U, Balmaseda MA, Balsamo G, Bauer P, Bechtold P, Beljaars ACM, van de Berg L, Bidlot J, Bormann N, Delsol C, Dragani R, Fuentes M, Geer AJ, Haimberger L, Healy SB, Hersbach H, Holm EV, Isaksen L, Kallberg P, Kohler M, Matricardi M, McNally AP, Monge-Sanz BM, Morcrette J-J, Park B-K, Peubey C, de Rosnay P, Tavolato C, Thepaut J-N,

- Vitar F (2011) The ERA-Interim reanalysis: configuration and performance of the data assimilation system. *Q J R Meteorol Soc* 137:553–597. doi:[10.1002/qj.828](https://doi.org/10.1002/qj.828)
- Dudhia J (1989) Numerical study of convection observed during the winter experiment using a mesoscale two-dimensional model. *J Atmos Sci* 46:3077–3107
- Engelbrecht FA, de Rautenbach CJW, McGregor JL, Katzfey JJ (2002) January and July climate simulations over the SADC region using the limited area model DARLAM. *Water SA* 28:361–373
- Evans JP, Westra S (2012) Investigating the mechanisms of diurnal rainfall variability using a regional climate model. *J Clim* 25:7232–7247. doi:[10.1175/JCLI-D-11-00616.1](https://doi.org/10.1175/JCLI-D-11-00616.1)
- Grell GA (1993) Prognostic evaluation of assumptions used by cumulus parameterizations. *Mon Weather Rev* 121:764–787
- Grell GA, Dévényi D (2002) A generalized approach to parameterizing convection combining ensemble and data assimilation techniques. *Geophys Res Lett*. doi:[10.1029/2002GL015311](https://doi.org/10.1029/2002GL015311)
- Hernandez-Diaz L, Laprise R, Sushama L, Martynov A, Winger K, Digas B (2013) Climate simulation over CORDEX Africa domain using the fifth-generation Canadian regional climate model (CRCM5). *Climate Dyn* 40:1415–1433. doi:[10.1007/s00382-012-1387-z](https://doi.org/10.1007/s00382-012-1387-z)
- Hong SY, Lim J-OJ (2006) The WRF single-moment 6-Class microphysics scheme (WSM6). *J Kor Meteorol Soc* 42:129–151
- Hong SY, Noh Y, Dudhia J (2006) A new vertical diffusion package with an explicit treatment of entrainment processes. *Mon Weather Rev* 134:2318–2341
- Huffman GJ, Adler RF, Morrissey M, Bolvin DT, Curtis S, Joyce R, McGavock B, Susskind J (2001) Global precipitation at one-degree daily resolution from multi-satellite observations. *J Hydrometeorol* 2:36–50
- Janjic ZI (1994) The step-mountain eta coordinate model: further developments of the convection, viscous sublayer, and turbulence closure schemes. *Mon Weather Rev* 122:927–945
- Joubert AM, Katzfey JJ, McGregor JL, Ngunyen KC (1999) Simulating midsummer climate over southern Africa using a nested regional climate model. *J Geophys Res* 104:19015–19025
- Kain JS (2004) The Kain–Fritsch convective parameterization: an update. *J Appl Meteor* 43:170–181
- Kgatuke MM, Landman WA, Beraki A, Mbedzi MP (2008) The internal variability of the RegCM3 over South Africa. *Int J Climatol* 28:505–520
- Leduc M, Laprise R (2009) Regional climate model sensitivity to domain size. *Clim Dyn* 32:833–854. doi:[10.1007/s00382-008-0400-z](https://doi.org/10.1007/s00382-008-0400-z)
- Ma LM, Tan ZM (2009) Improving the behavior of the cumulus parameterization for tropical cyclone prediction: convection trigger. *Atmos Res* 92:190–211. doi:[10.1016/j.atmosres.2008.09.022](https://doi.org/10.1016/j.atmosres.2008.09.022)
- Marshall JH, Dixon N, Garcia-Carreras L, Lister GMS, Parker DJ, Knippertz P, Birch C (2013) The role of moist convection in the West African monsoon system: Insights from continental-scale convection-permitting simulations. *Geophys Res Lett* 40. doi:[10.1002/grl.50347](https://doi.org/10.1002/grl.50347)
- Mason SJ, Jury MR (1997) Climatic variability and change over southern Africa: a reflection on underlying processes. *Prog Phys Geogr* 21:23–50
- Mlawer E, Taubman S, Brown P, Iacono M, Clough S (1997) Radiative transfer for inhomogeneous atmosphere: RRTM, a validated correlated-k model for the long-wave. *J Geophys Res* 102:16663–16682
- Nikulin G, Jones C, Giorgi F, Asrar G, Büchner M, Cerezo-Mota R, Christensen BO, Déqué M, Fernandez J, Hänsler A, Van Meijgaard E, Samuelsson P, Bamba Sylla M, Sushama L (2012) Precipitation climatology in an ensemble of CORDEX-Africa regional climate simulations. *J Clim* 25:6057–6078. doi:[10.1175/JCLI-D-11-00375.1](https://doi.org/10.1175/JCLI-D-11-00375.1)
- Philippon N, Rouault M, Richard Y, Favre A (2012) The influence of ENSO on winter rainfall in South Africa. *Int J Climatol* 32:2333–2347. doi:[10.1002/joc.3403](https://doi.org/10.1002/joc.3403)
- Pohl B, Crétat J, Camberlin P (2011) Testing WRF capability in simulating the atmospheric water cycle over Equatorial East Africa. *Clim Dyn* 37:1357–1379. doi:[10.1007/s00382-011-1024-2](https://doi.org/10.1007/s00382-011-1024-2)
- Ratna SB, Ratnam JV, Behera SK, Rautenbach CJ, Ndarana T, Takahashi K, Yamagata T (2013) Performance assessment of three convective parameterization schemes in WRF for downscaling summer rainfall over South Africa. *Clim Dyn* (on line). doi:[10.1007/s00382-013-1918-2](https://doi.org/10.1007/s00382-013-1918-2)
- Ratnam JV, Behera SK, Masumoto Y, Takahashi K, Yamagata T (2012) A simple regional coupled model experiment for summer-time climate simulation over southern Africa. *Clim Dyn* 39:2207–2217. doi:[10.1007/s00382-011-1190-2](https://doi.org/10.1007/s00382-011-1190-2)
- Reason CJC, Jagadheesha D (2005) A model investigation of recent ENSO impacts over southern Africa. *Meteorol Atm Phys* 89:181–205
- Rouault M, Richard Y (2003) Intensity and spatial extension of drought in South Africa at different time scales. *Water SA* 29:489–500
- Rouault M, White SA, Reason CJC, Lutjeharms JRE, Jobbard I (2002) Ocean-atmosphere interaction in the Agulhas Current region and a South African extreme weather event. *Weather Forecast* 17:655–669. doi:[10.1175/1520-0434\(2002\)017<0655:OAITA>2.0.CO;2](https://doi.org/10.1175/1520-0434(2002)017<0655:OAITA>2.0.CO;2)
- Rouault M, Reason CJC, Lutjeharms JRE (2003) Underestimation of latent and sensible heat fluxes above the Agulhas Current in NCEP and ECMWF analyses. *J Clim* 16:776–782. doi:[10.1175/1520-0442\(2003\)016<0776:UOLASH>2.0.CO;2](https://doi.org/10.1175/1520-0442(2003)016<0776:UOLASH>2.0.CO;2)
- Rouault M, Sen Roy S, Balling RC Jr (2013) The diurnal cycle of rainfall in South Africa in the austral summer. *Int J Climatol* 33:770–777. doi:[10.1002/joc.3451](https://doi.org/10.1002/joc.3451)
- Simmons A, Uppala S, Dee D, Kobayashi S (2007) ERA-interim: new ECMWF reanalysis products from 1989 onwards. *ECMWF Newsllett* 110:25–35
- Skamarock WC, Klemp JB, Dudhia J, Gill DO, Barker DM, Duda M, Huang XY, Wang W, Powers JG (2008) A description of the advanced research WRF version 3. NCAR technical note, NCAR/TN2013475?STR, 123 pp
- Tadross M, Gutowski W Jr, Hewitson B, Jack C, New M (2006) MM5 simulations of interannual change and the diurnal cycle of Southern African regional climate. *Theor Appl Climatol* 86:63–80
- Tyson PD, Preston-White RA (2000) *The weather and climate of Southern Africa*. Oxford University Press, Southern Africa, ISBN:9780195718065, 396 pp
- Vigaud N, Pohl B, Crétat J (2012) Tropical-temperate interactions over southern Africa simulated by a regional climate model. *Clim Dyn* 39:2895–2916. doi:[10.1007/s00382-012-1314-3](https://doi.org/10.1007/s00382-012-1314-3)
- Williams C, Kniveton D, Layberry R (2010) Assessment of a climate model to reproduce rainfall variability and extremes over Southern Africa. *Theor Appl Climatol* 99:9–27